Thin Solid Films 592 (2015) 155–161

Contents lists available at ScienceDirect

Thin Solid Films

journal homepage: www.elsevier.com/locate/tsf

Magnetic field induced one-dimensional nano/micro structures growth on the surface of iron oxide thin film

Pawan Kumar [a], Rajesh Kumar [b,*], Heung-No Lee [b]

[a] Jaypee University of Information Technology, Waknaghat, Solan, 173234 Himachal Pradesh, India
[a] Gwangju Institute of Science and Technology, Gwangju 500712, Republic of Korea

ARTICLE INFO

Article history:
Received 17 March 2015
Received in revised form 21 July 2015
Accepted 30 August 2015
Available online 2 September 2015

Keywords:
Crystal growth
Magnetic materials
Thin films
Nanoparticles
Microstructure
Magnetic field
Oriented growth

ABSTRACT

The influence of external magnetic field on the morphology of α-Fe_2O_3 thin film formed at liquid–vapor interface has been investigated. Application of magnetic field during the growth of film resulted in the magnetic moment ordering of constituent nanoparticles. Thus formed α-Fe_2O_3 thin film was transferred to a glass substrate, which upon annealing converted into one dimensional (1D) nanostructured thin film due to the oriented attachment of magnetically ordered nanoparticles. The effect of dopants viz. Ni^{2+} and Co^{2+} on the directional growth, and magnetic properties of nanostructures has also been investigated. The Ni^{2+} and Co^{2+} doped α-Fe_2O_3 1D nanostructured thin films show superparamagnetic and ferromagnetic behavior, respectively, whereas undoped α-Fe_2O_3 film exhibits superparamagnetism. From the room temperature magnetization measurements of films, it is found that the magnetization depends upon the morphology and magneto-crystalline anisotropy attributes of the film nanostructures.

1. Introduction

Owing to outstanding electrical, magnetic and optical properties the nano/micro sized structures of iron oxide have attracted great attention as compared with the bulk counterparts [1–2]. Among iron oxides, hematite (α-Fe_2O_3) is typically nontoxic and environment friendly iron oxide with band gap $E_g = 2.1$ eV [3]. In the case of film, the morphology and size of constituent α-Fe_2O_3 nanoparticles have great impact on its physical and chemical properties. The nano/micron sized structures of α-Fe_2O_3 have applications in diverse fields including catalysis [4], sensors [5], lithium-ion batteries [6], and environment protection, etc. [7].

Since the nanomaterials exhibit shape and/or size dependent properties [8], therefore, various efforts have been made to synthesize one-dimensional iron oxide structures for specific applications [9]. Here, we quote some of the methods reported for the growth of one-dimensional (1D) iron oxide structures, such as solution method [10–11], thermal oxidation [12–14], forced hydrolysis [15–16], hydrothermal [17–18] chemical precipitation [19], and solvothermal method [20]. For practical applications, such as integrated devices, these one-dimensional nanostructures (nanowires and nanorods) should be grown on substrate to form vertically aligned arrays. Still now, despite of tremendous efforts, it is challenging to develop a simple and versatile way to form α-Fe_2O_3 thin film composing 1D structure. However, for the synthesis of structured iron oxide film, the magnetic field may be considered as one of the synthesis parameters alike to the temperature and pressure. The applied magnetic field is not sensitive to the surface charges and solution pH, therefore, it does not influence the reaction mechanism as the other parameters do (electric field or current).

There are few reports where the magnetic field has been employed for the synthesis and assemblies of 1D and two-dimensional (2D) aggregates. During synthesis, the applied magnetic field enhances the dipole–dipole interaction by decreasing the surface energy, which results in the directional growth along the easy axis of magnetization. The effect of magnetic field is more in the case of materials possessing higher magnetic susceptibility due to their easy formation in the system, which is due to the magnetic field effect on Gibbs free energy leading to tremendous impact on structures and properties of materials [21]. The spin state of ions in the crystal structure can be changed by applying magnetic field during the synthesis process. Applied magnetic field generates novel magnetic domains in sample. In literature also, the application of magnetic field is reported an elegant way to orient and assemble disordered structures into highly ordered structures [22–30]. Nowadays, magnetic fields have been widely employed in the nanomaterials research area [31–34]. The response of magnetic field is different for ferromagnetic, paramagnetic and diamagnetic materials. In the case of ferromagnetic/ferrimagnetic materials, the growth of nanostructures in the presence of weak magnetic fields can induce anisotropy leading to the formation of 1D growth of nanostructures in the easy magnetization direction. The field strength and orientation can be varied or kept

* Corresponding author.
E-mail address: rajesh.kumar@juit.ac.in (R. Kumar).

http://dx.doi.org/10.1016/j.tsf.2015.08.047
0040-6090/

constant, for each of these magnetic nanomaterials in space and time or in both. When the magnetic field is applied, the Brownian motion on the surface of the solution gets diminished due to magnetic field lines, and the applied magnetic field forces the nucleated nanoparticle to align along their easy axes parallel to magnetic field.

Here, we report the formation of nano/micro structures on the surface of α-Fe_2O_3 thin films by applying external magnetic field during the film formation process. Along with undoped α-Fe_2O_3 thin films, films doped with Ni^{2+} and Co^{2+} were also formed in the presence of external magnetic field. The effect of Ni^{2+} and Co^{2+} doping on the morphology and magnetic properties of the formed iron oxide structures is studied. The as prepared nanostructured thin films were studied for structural, morphological and magnetic properties. The present study gives a new method of directional growth of one dimensional nanostructures, opening up a new way for controlled synthesis of nanostructured thin films with various dimensionalities and morphologies.

2. Experimental

Initially, a precursor solution containing 24 mM $FeCl_2$, 22 mM $FeCl_3 \cdot 6H_2O$ and 64 μM of polyvinyl alcohol (PVA) was formed. The measured pH value of solution was 2.8. The solution was placed in an ice-chamber to reduce the thermal fluctuations [35]. After cooling the solution, an out of plan magnetic field (~0.8 T) was applied on the surface of solution by using an electromagnet (with poles diameter 2 in.). A gap of 2.5 mm was kept between the solution surface and electromagnetic pole. Then to form a thin film on the surface of solution, NH_3 vapor (6 volume %) was introduced into the chamber. The NH_3 vapor interacts with the Fe^{3+} ions in precursor solution residing on the surface, and forms an iron oxide-poly vinyl alcohol (PVA) composite thin film (as shown in schematic of Fig. 1). The obtained film was transferred to the glass substrate, and then annealed at 500 °C in a horizontal tube furnace.

The thin film formation method, described above, was also applied to obtain doped (Ni^{2+} and Co^{2+} doping) iron oxide nanostructured thin films. The salts of $NiCl_2$ and $CoCl_2$ were taken in 15 molar percent, and added to the precursor solution, in two separate experiments. Thus obtained undoped and doped iron oxide thin films were also formed for horizontal magnetic field (in plane). Finally, these nanostructured thin films were characterized for structural properties by using X-ray Diffraction (XRD, PANanalytical X'pert-PRO) employing Cu Kα (λ = 1.5406 Å, 2θ = 20 to 60°) radiation, and for morphological study using Scanning Electron Microscopy (SEM, Hitachi, S-4700). The elemental composition and magnetic properties of the prepared samples were analyzed by Energy Dispersive X-ray spectroscopy (EDX,

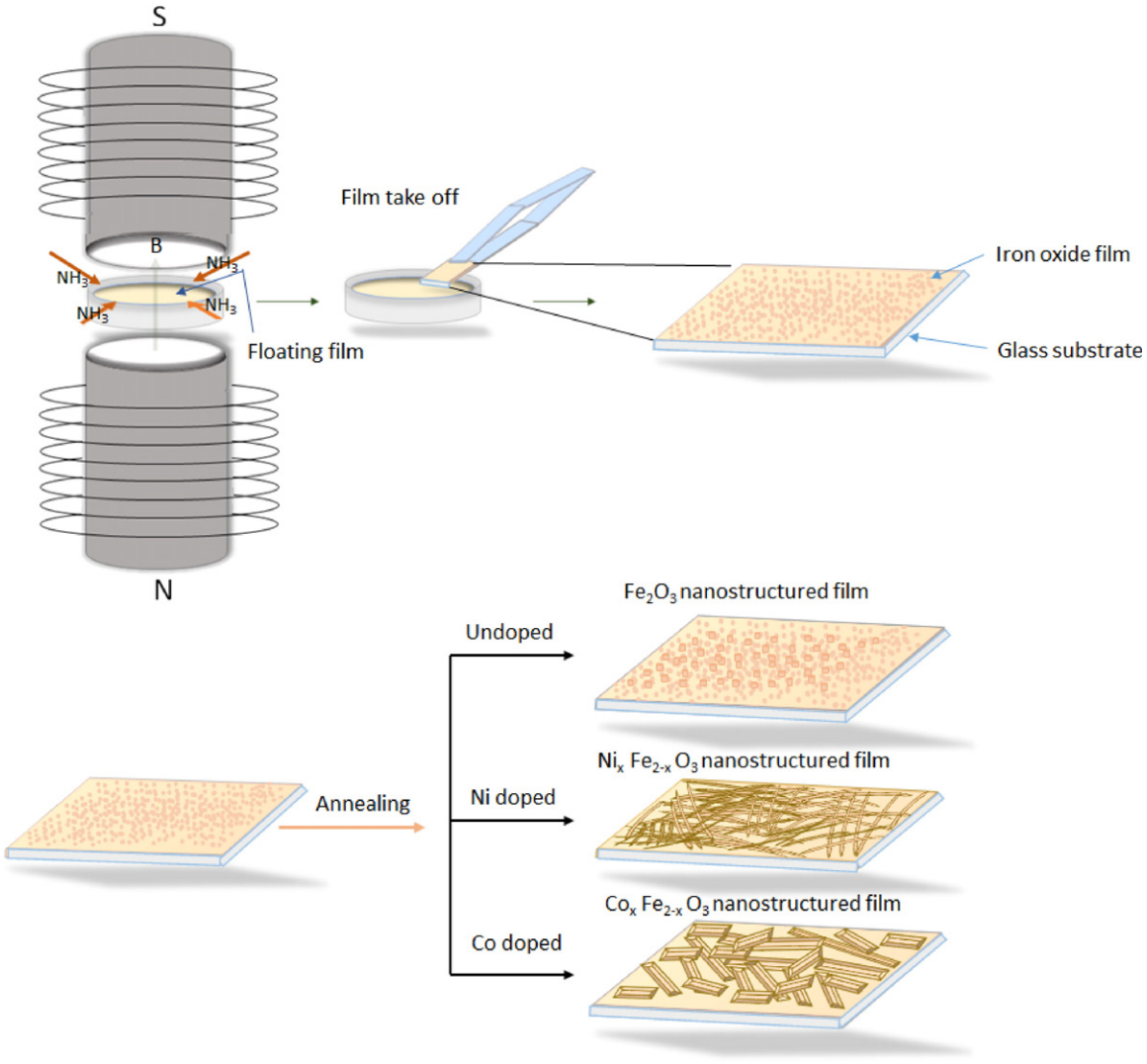

Fig. 1. Schematic presentation of the thin film formation process at the surface of solution in the presence of magnetic field (B) and ammonia (NH_3) vapor.

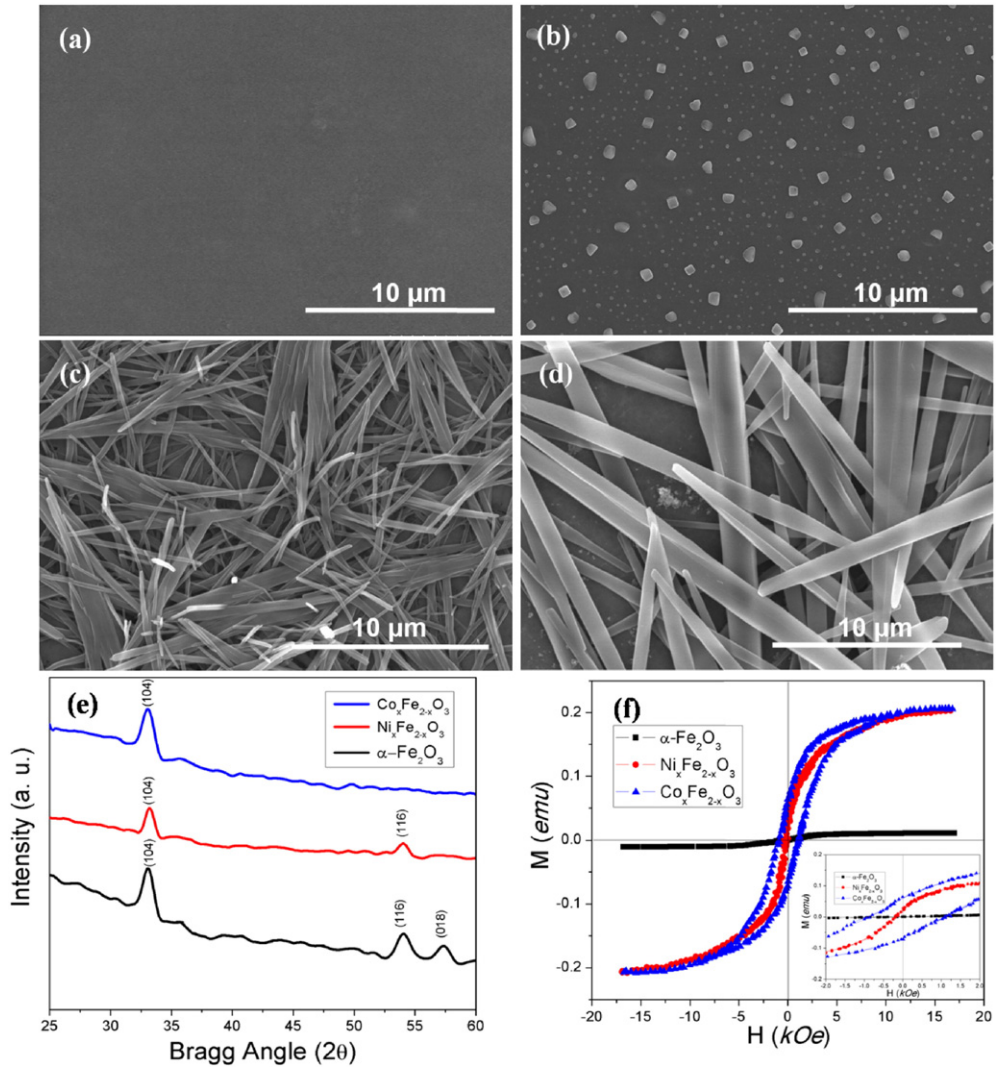

Fig. 2. SEM images of iron oxide thin films formed (a) without magnetic field, (b) with magnetic field (out of plane), (c) 15% Ni^{2+} doping with magnetic field applied, (d) 15% Co^{2+} doping with magnetic field applied and (e) XRD, and (f) VSM of the corresponding films (inset shows the magnetic behavior at the low magnetic field). All the films were annealed at 500 °C.

Oxford instruments, INCA PENTA FETX3) and Vibrating Sample Magnetometer (VSM) PAR 155.

3. Results and discussion

To estimate the effect of applied magnetic field, iron oxide thin films were formed both in the absence, and presence of external magnetic field. Fig. 2(a) and (b) shows the iron oxide thin film formed in the absence and presence of external magnetic field, respectively. The magnetic field was applied out of plane on the liquid–vapor interface. The films formed in the presence of external magnetic field possessing nanostructures (Fig. 2(b)) indicate that the external magnetic field has an effect on the surface morphology of the film. The iron oxide thin film is composed of nano and micrometer size particles. However, we observed that before annealing, both of the films that are formed in the absence and in the presence of magnetic field have similar surface morphology. But when annealed, the surface of the latter covered with nanostructured, whereas the former remained the same. Since the change in surface morphology appeared only after annealing, therefore, it may be inferred that the applied magnetic field has an effect on the magnetic moments of nanoparticles during the formation of film, which upon annealing resulted in nanostructured surface. The magnetic moment of iron oxide film can be enhanced by adding Ni^{2+} and Co^{2+} in the film [36–37]. In the present study, we also included Ni^{2+} and Co^{2+} ions in the precursor solution, and investigated their magnetic moment's effect on the morphology of iron oxide films. Fig. 2(c) shows the SEM image of Ni^{2+} doped iron oxide thin film. In this case, one dimensional nanostructures can be observed on the top of the film, whereas the film formed without any doping has nanoparticles on its surface. The Ni^{2+} in this case enhanced magnetic moment of nanostructures, and leaded to one dimensional form of nanostructures. Similar results were observed in the case of Co^{2+} doping. However, in the case of Co^{2+} doping, the surface was covered with microstructures as shown in Fig. 2(d).

Fig. 2(e) is XRD intensity patterns corresponding to undoped, Ni^{2+} and Co^{2+} doped iron oxide thin films. From the XRD pattern, it is observed that all the films are well crystalline, and match their diffraction peaks with those of α-Fe_2O_3 (JCPDS no. 89-8104). Also, there is no other secondary phase due to Ni^{2+} and Co^{2+} doping. The crystalline size calculated using Scherrer's formula, $D_{hkl} = 0.9/\beta \cos\theta$ is 6.7 nm,7 nm and 6.3 nm for α-Fe_2O_3, Ni^{2+} and Co^{2+} films, respectively. To study the magnetic behavior of the fabricated films, the M-H measurements were performed at room temperature. The M-H curve of undoped and doped iron oxide thin films is shown in Fig. 2(f). Both the undoped and Ni^{2+} doped samples show superparamagnetic behavior. In the magnetic curves, the undoped sample saturates at 7.95×10^5 A/m (or 10,000 Oe, as shown in the graph), whereas Ni^{2+} doped sample saturates above than 13.5×10^5 A/m (or 17,000 Oe). Also, the

magnetization value in the case of Ni^{2+} doped sample is higher than undoped sample. In the case of Co^{2+} doped sample, a ferromagnetic behavior with relatively larger coercivity value of 7.95×10^4 A/m (or 1000 Oe), and larger remanence is observed. The observed higher coercivity and remanence in Co^{2+} doped sample are attributed to enhanced shape of structures and related magneto-crystalline anisotropy [38]. We know that the magnetic iron oxide film doped with Co^{2+} ions has a stronger spin-order interaction than Fe^{2+} ions [39]. The doping of Co^{2+} ions decompensates the antiferromagnetic order of the lattice, which leads to an enhanced effective magnetic field seen by the Fe^{3+} nucleus [40]. Due to higher value of magneto-crystalline anisotropy of Co^{2+} ion, the post synthesis annealing resulted in large directional growth of nanostructure which prevented them from magnetizing in the directions other than that along their easy magnetic axes, leading to a higher directional growth and coercivity. The presence of Ni^{2+} and Co^{2+} was confirmed by EDX analysis. Fig. 3 shows the EDX of Ni^{2+} and Co^{2+} doped structures, these nanostructures have Ni^{2+} and Co^{2+} with the atomic percent of 15 and 14, respectively.

In literature, different magnetic behaviors of α-Fe_2O_3 nanostructure are reported. There are few studies [41,42], which indicate α-Fe_2O_3 nanostructures synthesized via sol–gel and hydrothermal methods to be superparamagnetic. However, the other studies report that α-Fe_2O_3 nanostructures are ferromagnetic [43,44]. In this study, we have obtained undoped and Ni^{2+} doped α-Fe_2O_3 structures which show superparamagnetic behavior, and doped with Co shows ferromagnetic behavior. In our case, the undoped thin film has small size of α-Fe_2O_3 nanocrystals, which should have uncompensated surface spin at their boundaries. The uncompensated spins lead the undoped α-Fe_2O_3 thin film to be superparamagnetic.

In the case of Co doping, due to smaller ionic radii of cobalt (72 pm), as compare with iron (74 pm), it may occupy the interstitial positions or sit on the grain boundaries. The XRD data indicates polycrystalline nature of the sample, possessing large number of grain boundaries. Here, the Co atoms will destroy the crystalline structure, which results into a decreased crystalline size, and therefore disappearance of the (116) and (018) peaks from the data. The Co with electronic configuration [Ar] $3d^74s^2$ has one electron in excess than Fe ([Ar] $3d^64s^2$) which has less energy of *d* state. When Co^{2+} with spin down electron substitutes Fe^{3+} ion, the spin down *d* band gets completely filled with remaining one *d* electron in the spin up band, which results in a net magnetization of 1 μ_B [45]. The increase in the magnetization value of Co-doped Fe_2O_3 takes place due to the canting of spin structure. The canting of spin structure is created by the imbalance resulted from the incorporation of Co^{2+} in Fe_2O_3 lattice [46]. A similar increased magnetization value behavior has been observed by Wieslaw A. Kaczmarek et al. (1996) [47]. The canting of spin produces an uncompensated magnetic moment of Fe^{3+} cation, resulting in a ferromagnetic behavior of the sample.

Similarly, in the case of Ni doping, the *d* bands of Ni ($3d^84s^2$) have lower energy than those of Fe. Here, the five *d* states in the down spin channel are occupied, and the remaining two *d* electrons are on the t_{2g} states of the Ni^{2+} site which are 2/3 filled. The local moment on the Ni^{2+} is 3 μ_B, and is polarized in the same direction as that of substituted Fe^{3+}, which gives a net magnetic moment of 2 μ_B in the direction opposite to the magnetic moment of the substituted Fe^{3+} [45]. The increase in the saturation magnetization of Ni^{2+} substituting at Fe^{3+} sites is due to the higher surface spins of electron. This occurs due to the increase in surface spin that causes an enhancement of the magnetization of antiferromagnetic nanoparticles. The over occupancy of Ni^{2+} ions in the tetrahedral sites of α-Fe_2O_3 creates more dense structure of pinning centers and discourages irreversible domain wall movement, and decreases the coercivity of Ni^{2+} doped α-Fe_2O_3 [45] resulting in a superparamagnetic thin film.

To estimate the effective direction of applied magnetic field, which give rise to the structured surface morphology of the film, we also investigated the effect of magnetic field which was applied parallel (in plane) to the liquid–vapor interface. Fig. 4(a) shows the corresponding SEM images of α-Fe_2O_3 thin film formed in the presence of magnetic field applied parallel to the liquid–vapor interface; the corresponding film obtained after annealing is shown in Fig. 4(b).

The formation of worm like nanostructures of α-Fe_2O_3 on the film surface took place after annealing the Ni^{2+} and Co^{2+} doped samples (Fig. 4(c) and (d)). The worm like structures are formed due to the crack formation on the film surface during the synthesis process in the presence of external (in plane) magnetic field, and size of the nanostructures changed due to the change in magnetic moment by doping.

4. Mechanism of the nano/micro structure formation

To ensure the formation of structures on the film surface due to annealing, we investigated thin film samples at different annealing temperatures. For this study, Co^{2+} doped iron oxide thin film was selected, and annealed at 100, 300 and 500 °C temperature. Fig. 5 shows SEM images of films formed after annealing at different temperatures. From the SEM images, it can be seen that without annealing, no nanostructure protudes on the film surface (Fig. 5(a)) but for the film annealed at 100 °C, small grains started to agglomerate on the film surface as shown in Fig. 5(b). For 300 °C of annealing temperature, one dimensional structures emerge out of the film surface (Fig. 5(c)), which enhanced to a length of micrometers at 500 °C as shown in Fig. 5(d). These results show that the growth of nanostructure takes place during the annealing process, and the applied magnetic field induces a directional magnetic moment inside the oxide nanoparticles during the formation of film.

The effect of external magnetic field on the magnetic moment of nucleated nanoparticles can be understood in the following way. We know that the magnetic force F(z) on metal ions at a position z is expressed by [40];

$$F(z) = \chi n H(z) \frac{\partial H(z)}{\partial z}. \quad (1)$$

Where n is number mole of Fe ions, χ is magnetic susceptibility, and H(z) is applied magnetic field. When magnetic field is employed on

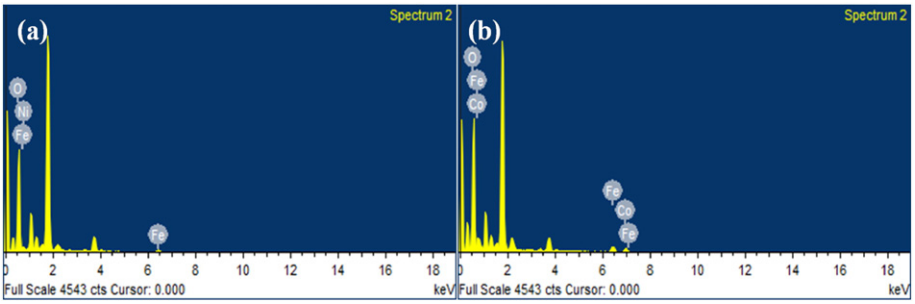

Fig. 3. The EDX of (a) Ni^{2+} doped and (b) Co^{2+} doped α-Fe_2O_3 structure formed on the surface of thin film.

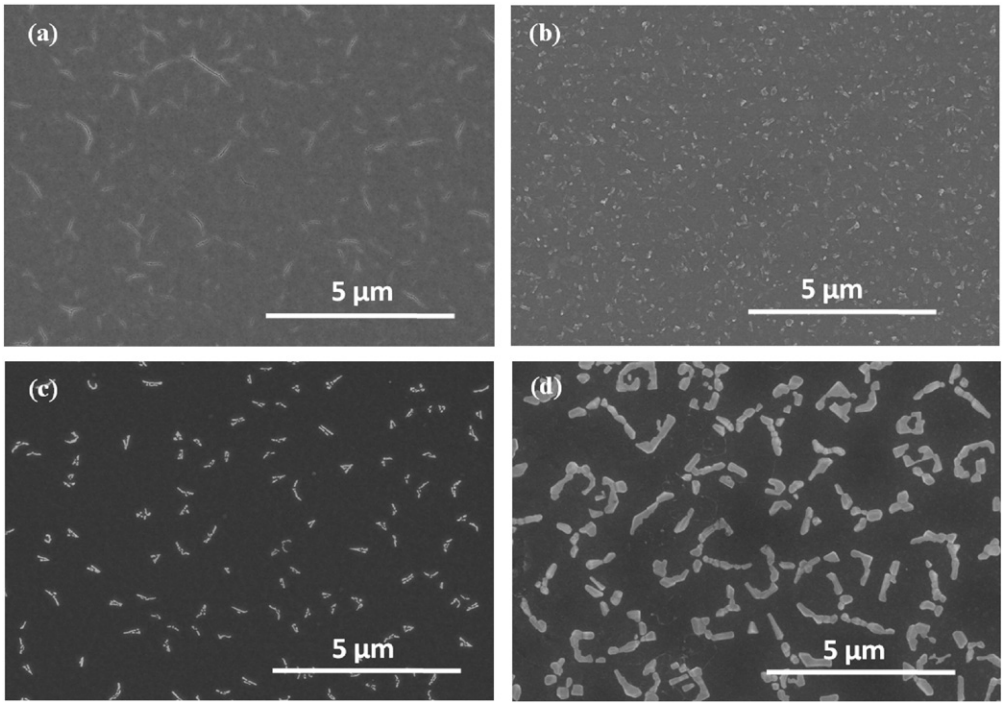

Fig. 4. The SEM images of α-Fe_2O_3 thin films (a) un-annealed and (b) annealed at 500 °C (c) 15% Ni^{2+} doped α-Fe_2O_3, and (d) 15% Co^{2+} doped α-Fe_2O_3 formed with the external magnetic field applied parallel (in plane) to the liquid–vapor interface.

liquid–vapor interface, it creates a change in the transport of Fe^{3+} ion and changes the Gibbs free energy of the reaction.

When a magnetic field is applied in a solution phase, the Fe^{3+} ions preferentially migrate and start to agglomerate along the magnetic line of force due to magnetic attraction, and the reaction occurs along the magnetic line of force. Thus the grain orientation of materials with magnetic anisotropy can be enhanced by applying a magnetic field as the material in the presence of magnetic field will produce magnetic energy [40]. The difference in magnetization directions produces different magnetic energy. The energy difference could be described as [40]:

$$\Delta E = -\frac{1}{2\mu_o}\Delta\chi VB^2. \quad (2)$$

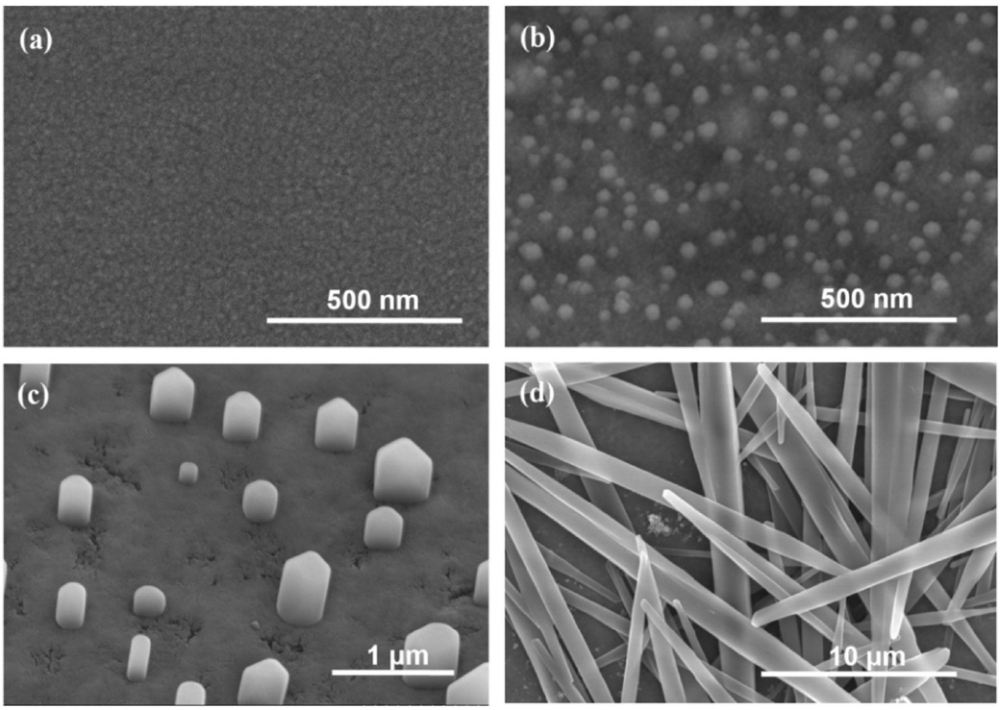

Fig. 5. SEM images of Co^{2+} doped iron oxide thin films (a) un-annealed, and annealed at (b) 100 °C, (c) 300 °C and (d) 500 °C temperature.

This orientation effect of a magnetic field is applicable to all (ferromagnetic/ferrimagnetic material, paramagnetic and diamagnetic) materials.

If the magnetic anisotropy is greater than the thermal energy, nucleated units will orientate with easy axes parallel to the applied field. For ferromagnetic and paramagnetic materials ($\chi > 0$), the largest magnetic susceptibility direction is parallel to the magnetic field direction and opposite for diamagnetic ($\chi < 0$) materials. Obviously, the orientation effect is associated with magnetic anisotropy and magnetic field intensity which influence the free energy (ΔG_M) of a chemical reaction, as given by [40]:

$$\Delta G_M = -\frac{1}{2}\mu_o(\Delta\chi_M)H^2. \quad (3)$$

Here, $\Delta\chi_M$ is the change in the susceptibility during reaction. The applied magnetic field determines the direction of any chemical change by controlling the ΔG_M. The generation of magnetic field effect is also due to the Zeeman interaction of the unpaired electron spins in Fe^{3+} ions with an external magnetic field. The increases length (L) in the presence of the applied magnetic field is given by the equation [48]:

$$L = L_o + \delta L\left(1 - e^{-\alpha H_{app}}\right). \quad (4)$$

This equation shows dependence of L on the Boltzmann distribution factor '$e^{-\alpha Happ}$' i.e. the ratio of Zeeman energy over thermal energy (αH_{app}). Zeeman energy of Fe^{3+} ions being in competition with the thermal activation energy in the presence of magnetic field [40] results to the nucleation of nanoparticles in the direction of easy axis that can minimize the energy of magnetization vector of material. Therefore, applied magnetic field might induce nucleation of α-Fe_2O_3 grains along the easy magnetic axis, which upon annealing results in the formation of 1D nanostructure due to orientation arrangement. The 1D nanostructure results due to the oriented growth of materials determined by the surface energy of the material and experimental conditions.

The overall growth mechanism of 1D structure formation can be understood schematically by Fig. 6. Initially, when no magnetic field is applied, the iron oxide grains have magnetic moments oriented in the random direction, which after annealing do not show a directional growth (Fig. 6(a)). But when an external magnetic field is applied during the film formation, the nucleated grains might be having their magnetic moments aligned in the direction of magnetic field as shown in Fig. 6(b). These films upon annealing give directional growth due to oriented attachment of nanoparticles [49] as shown in Fig. 6(d).The high temperature annealing, evaporates PVA content from the film, and the magnetized grains arrange themselves to reduce their magneto-crystalline anisotropy energy, and results in a directional growth of the nanostructures.

5. Conclusions

Nano/micro structures are produced on the surface of thin film due to the application of magnetic field. The applied magnetic field produces an effect on the magnetic moment of nucleated iron oxide nanoparticles inside the film. The induced magnetic moment of nanoparticles align them along the direction of applied magnetic field, and upon annealing an oriented attachment nanoparticles form one dimensional structure on the film surface. Thus formed α-Fe_2O_3 and Ni^{2+} doped α-Fe_2O_3 films are superparamagnetic, whereas Co^{2+} doped film is ferromagnetic. The magnetic moment of α-Fe_2O_3 film is successfully enhanced with the doping of Ni^{2+} and Co^{2+} ions. A larger value of magneto-crystalline anisotropy in Co^{2+} doped samples as compared with undoped and Ni^{2+} doped iron oxide films results in enlargement of 1D structures on the film surface.

Acknowledgments

This work was supported by nanotechnology research grant of Jaypee University of Information Technology and the National Research Foundation of Korea (NRF) grant funded by the Korean government (NRF-2015R1A2A1A05001826).

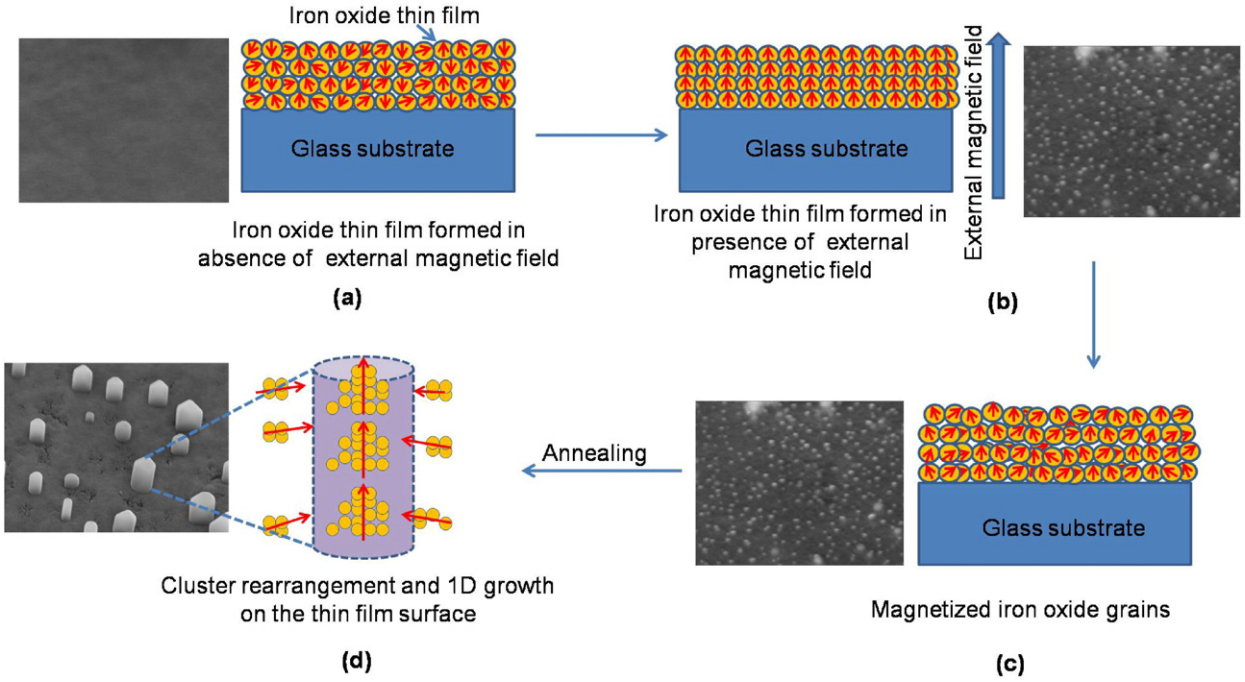

Fig. 6. Schematic of nanostructures formation mechanism on the surface of iron oxide thin film in the presence of external magnetic field.

References

[1] A.M. Xavier, F.F. Ferreira, F.L. Souza, Morphological and structural evolution from akaganeite to hematite of nanorods monitored by ex situ synchrotron X-ray powder diffraction, RSC Adv. 4 (2014) 17753.

[2] Y.M. Zhao, Y.H. Li, R.Z. Ma, M.J. Roe, D.G. McCartney, Y.Q. Zhu, Growth and characterization of iron oxide nanorods/nanobelts prepared by a simple iron–water reaction, Small 2 (2006) 422–427.

[3] X. Wen, S. Wang, Y. Ding, Z.L. Wang, S. Yang, Controlled growth of large-area, uniform, vertically aligned arrays of α-Fe_2O_3 nanobelts and nanowires, J. Phys. Chem. B 109 (2005) 215–220.

[4] J.Y. Kim, G. Magesh, D.H. Youn, J.W. Jang, J. Kubota, K. Domen, J.S. Lee, Single-crystalline, wormlike hematite photoanodes for efficient solar water splitting, Sci. Rep. 3 (2013) 2681.

[5] V.V. Jadhava, S.A. Patil b, D.V. Shindeb, S.D. Waghmarea, M.K. Zatea, R.S. Manea, S.-H. Hanb, Hematite nanostructures: morphology-mediated liquefied petroleum gas sensors, Sensors Actuators B 188 (2013) 669–674.

[6] J. Zhu, K.Y. Simon Ng, D. Deng, Hollow cocoon-like hematite mesoparticles of nanoparticle aggregates: structural evolution and superior performances in lithium ion batteries, ACS Appl. Mater. Interfaces 6 (2014) 2996–3001.

[7] H. Liang, X. Xu, W. Chen, B. Xuab, Z. Wang, Facile synthesis of hematite nanostructures with controlled hollowness and porosity and their comparative photocatalytic activities, Cryst. Eng. Commun. 16 (2014) 959–963.

[8] J. Velev, A. Bandyopadhyay, W.H. Butler, S. Sarker, Electronic and magnetic structure of transition-metal-doped α-hematite, Phys. Rev. B 71 (2005) 205208.

[9] J.S. Chen, T. Zhu, C.M. Li, X.W. Lou, Building hematite nanostructures via oriented attachment, Angew. Chem. Int. Ed. 50 (2011) 650.

[10] K. Woo, H.J. Lee, J.P. Ahn, Y.S. Park, Sol–gel mediated synthesis of Fe_2O_3 nanorods, Adv. Mater. 15 (2003) 1761.

[11] M.G. Sung, K. Sassa, T. Tagawa, T. Miyata, H. Ogawa, M. Doyama, S. Yamada, S. Asai, Application of a high magnetic field in the carbonization process to increase the strength of carbon fibers, Carbon 40 (2002) 2013–2020.

[12] H. Zhou, S.S. Wong, A facile and mild synthesis of 1-D ZnO, CuO, and α-Fe_2O_3 nanostructures and nanostructured arrays, ACS Nano 2 (2008) 944.

[13] L. Yuan, R. Cai, J.I. Jang, W. Zhu, C. Wang, Y. Wang, G. Zhou, Morphological transformation of hematite nanostructures during oxidation of iron, Nanoscale 5 (2013) 7581.

[14] W. Merchan-Merchan, A.V. Saveliev, A.M. Taylor, High rate flame synthesis of highly crystalline iron oxide nanorods, Nanotechnology 19 (2008) 125605.

[15] S. Musić, S. Krehula, S. Popović, Ž. Skoko, Some factors influencing forced hydrolysis of $FeCl_3$ solutions, Mater. Lett. 57 (2003) 1096.

[16] Z. Pu, M. Cao, J. Yang, K. Huang, C. Hu, Controlled synthesis and growth mechanism of hematite nanorhombohedra, nanorods and nanocubes, Nanotechnology 17 (2006) 799–804.

[17] T.K. Van, H.G. Cha, C.K. Nguyen, S.W. Kim, M.H. Jung, Y.S. Kang, Nanocrystals of hematite with unconventional shape-truncated hexagonal bipyramid and its optical and magnetic properties, Cryst. Growth Des. 12 (2012) 862–868.

[18] Y.N. Li, P. Zhang, Z. Guo, H. Liu, Shape evolution of α-Fe_2O_3 and its size-dependent electrochemical properties for lithium-ion batteries, J. Electrochem. Soc. 155 (2008) A196.

[19] W.F. Tan, Y.T. Yu, M.X. Wang, F. Liu, L.K. Koopal, Shape evolution synthesis of monodisperse spherical, ellipsoidal, and elongated hematite (α-Fe_2O_3) nanoparticles using ascorbic acid, Cryst. Growth Des. 14 (2014) 157–164.

[20] G. Du, P. Liu, W. Guo, Y. Han, J. Zhang, Z. Jang, Z. Ma, J. Han, Z. Liu, K. Yao, The influence of high magnetic field on electric-dipole emission spectra of Eu^{3+} in different single crystals, J. Mater. Chem. C 1 (2013) 7608–7613.

[21] J.H. Wang, Y.W. Ma, K. Watanabe, Magnetic-field-induced synthesis of magnetic γ-Fe_2O_3 nanotubes, Chem. Mater. 20 (2008) 20–22.

[22] R.S.M. Rikken, R.J.M. Nolte, J.C. Maan, J.C.M. Hest, D.A. Wilsonb, P.C.M. Christianen, Manipulation of micro- and nanostructure motion with magnetic fields, Soft Matter 10 (2014) 1295.

[23] D. Fragouli, R. Buonsanti, G. Bertoni, C. Sangregorio, C. Innocenti, A. Falqui, D. Gatteschi, P.D. Cozzoli, A. Athanassiou, R. Cingolani, Dynamical formation of spatially localized arrays of aligned nanowires in plastic films with magnetic anisotropy, ACS Nano 4 (2010) 1873–1878.

[24] Y. Lu, Y.D. Yin, Y.N. Xia, Three-dimensional photonic crystals with non-spherical colloids as building blocks, Adv. Mater. 13 (2001) 415–420.

[25] T. Ding, K. Song, K. Clays, C.H. Tung, Fabrication of 3D photonic crystals of ellipsoids: convective self-assembly in magnetic field, Adv. Mater. 21 (2009) 1936–1940.

[26] K. Cheng, Q.W. Chen, Z.D. Wu, M.S. Wang, H. Wang, Colloids of superparamagnetic shell: synthesis and self-assembly into 3D colloidal crystals with anomalous optical properties, Cryst. Eng. Commun. 13 (2011) 5394–5400.

[27] H. Wang, Q.W. Chen, Y.F. Yu, K. Cheng, Assembly of superparamagnetic colloidal nanoparticles into field-responsive purple Bragg reflectors, Dalton Trans. 40 (2011) 4810 H. Wang, Y.F. Yu, Q.W. Chen, K. Cheng, Dalton Trans. 40 (2011) 559-563.

[28] H. Wang, Y.F. Yu, Q.W. Chen, K. Cheng, Carboxyl-functionalized nanoparticles with magnetic core and mesopore carbon shell as adsorbents for the removal of heavy metal ions from aqueous solution, Dalton Trans. 40 (2011) 559–563.

[29] H. Wang, Q.W. Chen, Y.F. Yu, K. Cheng, Y.B. Sun, Size and solvent-dependent magnetically responsive optical diffraction of carbon-encapsulated superparamagnetic colloidal photonic crystals, J. Phys. Chem. C 115 (2011) 11427.

[30] H. Hu, C. Chen, Q. Chen, Magnetically controllable colloidal photonic crystals: unique features and intriguing applications, J. Mater. Chem. C 1 (2013) 6013.

[31] W.L. Zhou, A. Kumbhar, J. Wiemann, J.Y. Fang, E.E. Carpenter, C.J. ÒConnor, Gold-coated iron (Fe@Au) nanoparticles: synthesis, characterization, and magnetic field-induced self-assembly, J. Solid State Chem. 159 (2001) 26–31.

[32] V. Raman, A. Bose, B.D. Olsen, T.A. Hatton, Long-range ordering of symmetric block copolymer domains by chaining of superparamagnetic nanoparticles in external magnetic fields, Macromolecules 45 (2012) 9373.

[33] A. Sinha, S. Nayar, B.K. Nath, D. Das, P.K. Mukhopadhyay, Magnetic field induced synthesis and self-assembly of super paramagnetic particles in a protein matrix, Colloids Surf. B 43 (2005) 7–11.

[34] H. Singh, P.E. Laibinis, T.A. Hatton, Rigid, superparamagnetic chains of permanently linked beads coated with magnetic nanoparticles. Synthesis and rotational dynamics under applied magnetic fields, Langmuir 21 (2005) 11500–11509.

[35] P. Kumar, R.K. Singh, N. Rawat, P.B. Barman, S.C. Katyal, H. Jang, H.N. Lee, R. Kumar, A novel method for controlled synthesis of nanosized hematite (α-Fe_2O_3) thin film on liquid–vapor interface, J. Nanoparticle Res. 15 (2013) 1532.

[36] J. Velev, A. Bandyopadhyay, W.H. Butler, S. Sarker, Electronic and magnetic structure of transition-metal-doped α-hematite, Phys. Rev. B 71 (2005) 205208.

[37] D. Tripathy, A.O. Adeyeye, C.B. Boothroyd, S.N. Piramanayagam, Magnetic and transport properties of Co-doped Fe_3O_4 films, J. Appl. Phys. 101 (2007) 013904.

[38] G.A. Petrakovskii, I. Pankrats, V.M. Sosnin, V.N. Vasil'ev, Effect of doping withCo^{2+} ions on the resonant and static magnetic properties of hematite, Sov. Phys. - JETP 58 (1983) 403.

[39] C. Saragovi, J. Arpe, E. Sileo, R. Zysler, L.C. Sanchez, C.A. Barrero, Changes in the structural and magnetic properties of Ni-substituted hematite prepared from metal oxinates, Phys. Chem. Miner. 31 (2004) 625.

[40] L. Hu, R. Zhang, Q. Chen, Synthesis and assembly of nanomaterials under magnetic fields, Nanoscale 6 (2014) 14064–14105.

[41] M. Tadić, D. Markovic, V. Spasojević, V. Kusigerski, M. Remškar, J. Pirnat, Z. Jagličić, Synthesis and magnetic properties of concentrated α-Fe_2O_3 nanoparticles in silica matrix, J. Alloys Compd. 441 (2007) 291–296.

[42] M. Tadić, M. Panjan, V. Damnjanovic, I. Milosevic, Magnetic properties of hematite (α-Fe_2O_3) nanoparticles prepared by hydrothermal synthesis method, Appl. Surf. Sci. 320 (2014) 183–187.

[43] M. Tadić, N. Čitaković, M. Panjan, Z. Stanojević, D. Markovic, D. Jovanovic, V. Spasojevic, Synthesis, morphology and microstructure and magnetic properties of hematite submicron particles, J. Alloys Compd. 509 (2011) 7639–7644.

[44] M. Tadić, N. Čitaković, M. Panjan, B. Stanojević, D. Markovic, D. Jovanovic, V. Spasojevic, Synthesis, morphology and microstructure of pomegranate-like hematite (α-Fe_2O_3) superstructure with high coercivity, J. Alloys Compd. 543 (2012) 118–124.

[45] J. Velev, A. Bandyopadhyay, W.H. Butler, S. Sarker, Electronic and magnetic structure of transition-metal-doped a-hematite, Phys. Rev. B 71 (205208) (2005).

[46] A. Akbar, S. Riaz, R. Ashraf, S. Naseem, Magnetic and magnetization properties of Co-doped Fe_2O_3 thin films, IEEE Trans. Magn. 50 (8) (2014) 2201204.

[47] W.A. Kaczmarek, Structural and magnetic properties of cobalt-doped iron oxide particles prepared by novel mechanochemical method, J. Magn. Magn. Mater. 157 (158) (1996) 264–265.

[48] R. Wang, P. Li, C. Chen, Template-free synthesis and self-assembly of aligned nickel nanochains under magnetic fields, J. Nanosci. Nanotechnol. 11 (2011) 1–5.

[49] B. Jia, L. Gao, Growth of well-defined cubic hematite single crystals: oriented aggregation and Ostwald ripening, Cryst. Growth Des. 8 (2008) 1372.